UDK 661.882:616.314
Original scientific article/Izvirni znanstveni članek

ISSN 1580-2949
MTAEC9, 56(4)429(2022)

ESTIMATION OF THE CORROSION PROPERTIES FOR TITANIUM DENTAL ALLOYS PRODUCED BY SLM

OCENA KOROZIJSKIH LASTNOSTI TITANOVIH DENTALNIH ZLITIN, IZDELANIH S SLM POSTOPKOM

Tadeja Kosec[1], Mirjam Bajt Leban[1], Maja Ovsenik[2,3], Matej Kurnik[2], Igor Kopač[2]*

[1]Slovenian National Building and Civil Engineering Institute, Ljubljana, Slovenia
[2]Medical Faculty, University of Ljubljana, Ljubljana, Slovenia
[3]Orthos, Ljubljana, Slovenija

Prejem rokopisa – received: 2022-06-09; sprejem za objavo – accepted for publication: 2022-07-07

doi:10.17222/mit.2022.519

Titanium alloys are known for their excellent biocompatible properties. The development of additive-manufacturing technologies has increased the interest in the use of Ti-6Al-4V, produced by selective laser melting (SLM) method, also in dentistry, i.e., prosthodontics and orthodontics. In the present paper, the effect of laser printing parameters in the selective laser melting (SLM) process on the porosity and corrosion behavior of Ti-6Al-4V dental alloy was metallographically and electrochemically studied. All the tests were performed in artificial saliva at 37 °C. Different forms of Ti-6Al-4V alloy were selected: a reference sample, i.e., pre-fabricated milling disc in wrought condition and four different 3D-printed samples made from Ti-6Al-4V powder using the SLM method, one being heat treated. Electrochemical, spectroscopic and hardness measurements were employed in the study. It was shown that the SLM-produced Ti-6Al-4V samples with different printing parameters have similar microstructural and electrochemical properties, while the electrochemical properties of a reference and thermally treated 3D-printed sample were different, most probably due to the change in the microstructure of the alloys. The corrosion properties were related to the microstructural properties as well as to the pore density.

Keywords: Ti-6Al-4V, dental alloys, artificial saliva, selective laser melting, corrosion

Titanove zlitine so znane po odličnih biokompatibilnih lastnostih. Razvoj aditivnih tehnologij je povečal zanimanje za uporabo Ti-6Al-4V, proizvedenega z metodo selektivnega laserskega taljenja (SLM) v zobozdravstvu - tako v protetiki kot v ortodontiji. V prispevku smo metalografsko in elektrokemijsko proučili vpliv parametrov laserskega tiska pri procesu selektivnega laserskega taljenja (SLM) na poroznost in korozijsko obnašanje dentalne zlitine Ti-6Al-4V. Vsi testi so bili opravljeni v umetni slini pri telesni temperaturi 37 °C. Izbrane so bile različne oblike zlitine Ti-6Al-4V: referenčni vzorec (v obliki diska za rezkanje v kovanem stanju) in štirje različni 3D natisnjeni vzorci iz prahu Ti-6Al-4V po metodi selektivnega laserskega taljenja (SLM), pri čemer je eden toplotno obdelan. Pri raziskavi so bile uporabljene elektrokemijske, spektroskopske metode in meritve trdote. Pokazalo se je, da imajo vzorci Ti-6Al-4V, izdelani s postopkom SLM, z različnimi parametri, podobne mikrostrukturne in elektrokemijske lastnosti, medtem ko so bile elektrokemijske lastnosti referenčnega in termično obdelanega 3D natisnjenega vzorca različne, najverjetneje zaradi različne mikrostrukture te zlitine. Korozijske lastnosti so bile povezane z mikrostrukturnimi lastnostmi, pa tudi z gostoto por.

Ključne beside: Ti-6Al-4V, dentalne zlitine, umetna slina, selektivno lasersko taljenje, korozija

1 INTRODUCTION

Titanium and titanium-based alloys are widely applied in biomedical and dental applications. They possess favorable mechanical properties such as high tensile strength, toughness and ductility.[1] The most important feature for biomedical and dental applicationd is thus their chemical inertness through corrosion resistance and biocompatible properties.[2]

In dentistry, Ti and titanium alloys are used for different applications, such as dental implants, crowns and bridges, posts and cores in prosthodontics and NiTi archwires in orthodontics.[3] With the recent rapid development of additive-manufacturing technologies, the selective laser melting (SLM) procedure replaces precision metal casting technology and is being employed in dentistry for custom-made options, rapid in-lab fabrication and lower material usage.[4]

The biocompatible properties of Ti and Ti alloys are due to a thin oxide layer that forms at the surface.[5] This oxide layer is approximately 2–5 nm thick, if grown natively upon exposure to air.[6] If grown in a corrosive solution such as simulated body fluid, its thickness was reported[7] to be 9 nm at 2.5 V, if fretted, thicker oxide forms in the anodic regime than in the cathodic regime.[8] In simulated saliva the oxides on Ti, Ti-6Al-4V and Ti-6Al-7Nb vary and reach up to 21 nm, while in the presence of 0.25 % NaF, the oxide thickness was reported to increase to 30 nm, studied by XPS.[9]

In general, the passive film consists of a dense inner layer and a porous outer layer, which was confirmed electrochemically and spectroscopically decades ago.[10–12] The thickness of the oxide layer can also be controlled by different processes like anodization, micro arc, laser,

*Corresponding author's e-mail:
igor.kopac@mf.uni-lj.si (Igor Kopač)

plasma and thermal oxidation.[6,13,14] The thickness of the oxide can be tailored with artificial passivation[6] in H_3PO_4, H_2O_2 or nitric acid, reaching thicknesses up to 400 nm by anodization in NaOH.

With the implementation of Ti-6Al-4V products, produced by selective laser melting, the need for knowledge of their mechanical, microstructural and corrosive behavior increases in order to understand differences and possible effects when compared to wrought alloys and cast procedures. The research in the field has increased immensely with different focuses in their studies: the effect of recycled powder, the position on the SLM printing board, the effect of laser power density and similar.

Titanium alloys comprising both α-Ti and β-Ti are most often used in aircraft. Ti-6Al-4V is the most common $\alpha + \beta$-Ti alloy, which possesses a high creep resistance and toughness (from the α-Ti) and high strength and fatigue resistance (from the β-Ti).[15,16] The microstructure is affected to a great extent by the production technology and post heat treatments.[17]

In this paper different laser powers and laser speeds, i.e., laser power densities, both as printed and heat treated, are studied and compared to the reference wrought alloy. The microstructural, physical and corrosion properties of the different forms of Ti-6Al-4V alloys were defined and compared. The effects of microstructure, porosity, and hardness were sought in relation to the properties of corrosion and performance.

2 EXPERIMENTAL PART

For samples produced by the SLM procedure, the Ti-6Al-4V powder was from S&S Scheftner GmbH as powder (Starbond Ti4Powder 45) with the chemical composition 89.0 *w*/% Ti, 6.0 *w*/% Al, 4.0 *w*/% V with N, C, H, Fe and O < 1.0 *w*/% . The following printing parameters were used: laser power 60 W, 75 W and 90 W with various travel velocities of 520 mm/s and 805 mm/s, with a hatch distance of 0.025 mm and a layer thickness 0.025 mm. The calculated energy density and sample description are given in **Table 1**. One sample was heat treated in argon at 1000 °C for 1 h and cooled down to 500 °C in the furnace, followed by cooling in the air. The reference sample of Ti-6Al-4V was supplied by Goodfellow in the wrought and annealed condition, with chemical composition consisting of 90.0 *w*/% Ti, 6.0 *w*/% Al and 4.0 *w*/% V.

Light microscopy on the metallographically prepared samples at different magnifications was executed using a Carl Zeiss metallographic microscope (Germany, 2009) to reveal the microstructure as well as the pore share at the cross-section of the samples (metallographic photographs were analyzed by ImageJ software to determine the percentage of porosity). The relative density was estimated by Archimedes' method in 96 % ethanol. Vickers hardness measurements (HV 0.3) were conducted according to the standard[18] ISO 6507-1: 2018 using a EMCO DuraScan 70 G5 hardness-testing machine (Austria, 2022).

Electrochemical tests were conducted using a Gamry ref 600+ Potentiostat/Galvanostat (USA, 2015). First, the open-circuit potential (OCP) was measured for at least 1 h, or until a steady state was reached. Linear polarization measurements followed at a scan rate of 0.1 mV/s in the potential range ± 20 mV vs E_{corr} (results not shown in this study). Electrochemical impedance spectroscopy measurements were then conducted by measuring the impedance at frequencies between 65 kHz and 1 mHz, applying a perturbation signal of 20 mV and measuring 7 points per decade. Finally, potentiodynamic measurements were executed, starting –250 mV cathodically vs E_{corr}, progressing in the anodic direction up to 3.2 V or 1 mA/cm^2 at a scan rate of 1 mV/s. Then, the electrochemical parameters were extracted from electrochemical measurements using Echem Analyst Software.

The corrosion cell for the electrochemical tests consisted of an assembly of three electrodes in a jacked cell with a volume of V = 350 cm^3, using an Ag/AgCl reference electrode and a graphite rod as a counter electrode. The areas of the working electrodes were 0.64 cm^2 for the 3D-printed samples and 0.785 cm^2 for a reference sample in the form of a disc with 15 mm diameter. All the results presented were normalized.

Artificial saliva[14] was prepared to contain 0.6 g/L NaCl, 0.72 g/L KCl, 0.22 g/L $CaCl_2 \cdot 2\ H_2O$, 0.68 g/L KH_2PO_4, 0.856 g/L $Na_2HPO_4 \cdot 12\ H_2O$, 0.060 g/L KSCN, 1.5 g/L $KHCO_3$ and 0.03 g/L citric acid with a pH 6.5. All the measurements were conducted at 37 °C.

All the specimens were wet grinded with 1200–grit SiC emery paper and afterwards ultrasonically cleaned in acetone for 3 min.

Table 1: Investiated Ti-6Al-4V samples

Ti-6Al-4V sample	Laser power (W)	Laser speed (mm/s)	Energy (J/mm^3)
SLM-60-520	60	520	132
SLM-75-805	75	805	106
SLM-75-805-HT (heat treated)	75	805	106
SLM-90-520	90	520	198
Ti-6Al-4V-reference	–	–	–

3 RESULTS AND DISCUSSION

3.1 Microstructure, porosity and hardness

First, the SLM-manufactured Ti-6Al-4V samples were metallographically prepared (**Figure 1**). The microstructural investigation is presented in **Figure 1** and the porosity study is presented in **Figure 2** using light microscopy.

The microstructures of the SLM-fabricated samples are similar, regardless of the different printing parameters and consist of martensite (α'), as can be observed from **Figure 1c**. The inset in **Figure 1b** presents a

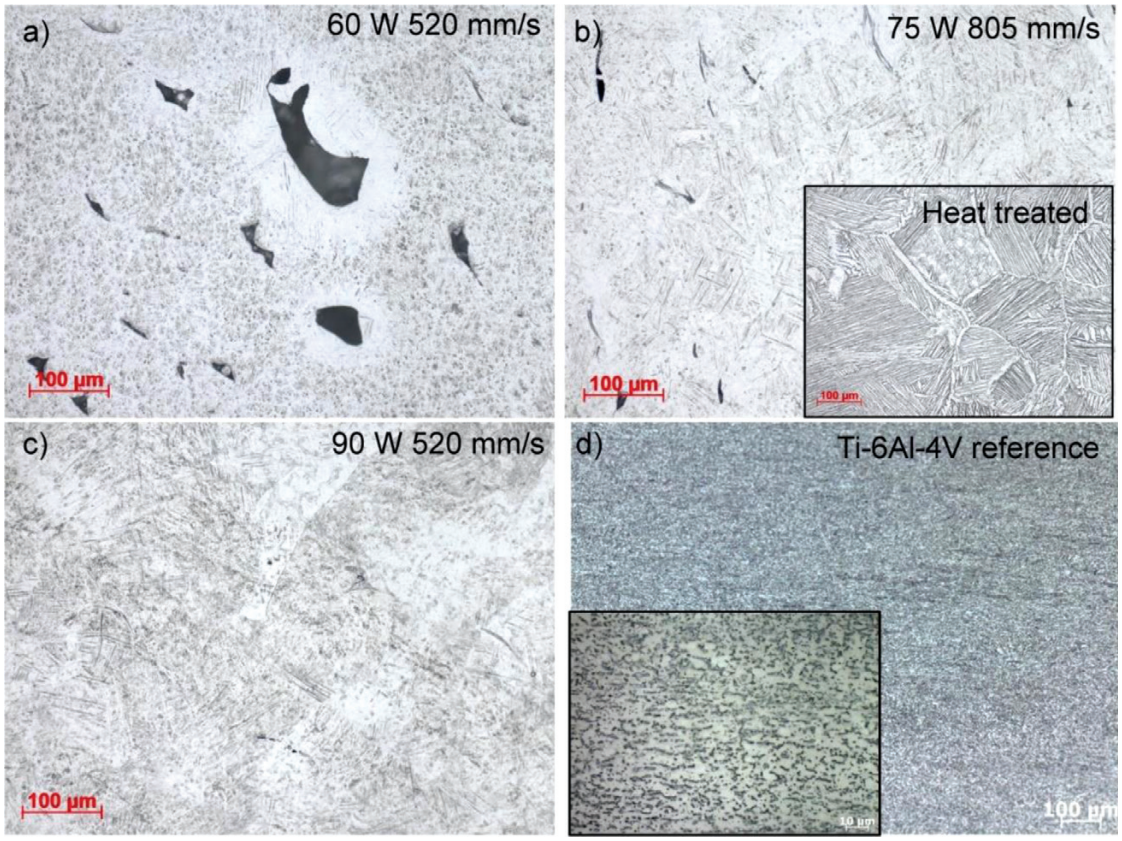

Figure 1: Metallographic study of different 3D-printed Ti-6Al-4V samples and reference alloy observed at 100× and 200× magnifications

heat-treated sample where a more defined microstructure is observed. A previous martensitic microstructure underwent temperature transformation above β-transus and during cooling to the room temperature, it transformed to the so-called Widmanstatätten/basket-weave microstructure consisting of α-phase lamellas separated by β plates within large (100–250 µm) primary β grains and α-phase along the grain boundaries.[22] The reference sample in **Figure 1d** consisted of globular $\alpha + \beta$ microstructure (dark regions represent β-phase), typical for a wrought Ti-6Al-4V alloy in the annealed condition.

The porosity of each sample was defined at a 12.5× magnification with image analysis using ImageJ software according to the standard ASTM E2109-01.[19] Hardness measurements were then executed with a minimum of six measurements taken for each sample. The results of the porosity, relative density determined by Archimedes' method and hardness are presented in **Table 2**.

All the observed SLM-manufactured Ti-6Al-4V samples were very rough at the surface since no post surface treatment was made at the supplier. The porosity of the SLM printed samples is related to the laser power density. Lower laser-power densities (samples SLM-60-520 and SLM-75-805) resulted in a higher porosity. For these two samples it was 0.4 % and 0.5 %, respectively. The lowest laser-power density and heat treatment for sample SLM-75-805, as well as the highest laser-power density resulted (SLM-60-520) in the lowest porosity of 0.1 % (**Figures 2c** and **2d**). The relative density, estimated by Archimedes' method, was the highest for the heat treated SLM-75-805, which indicates the lowest porosity as determined by microscopic method. On the other hand, the

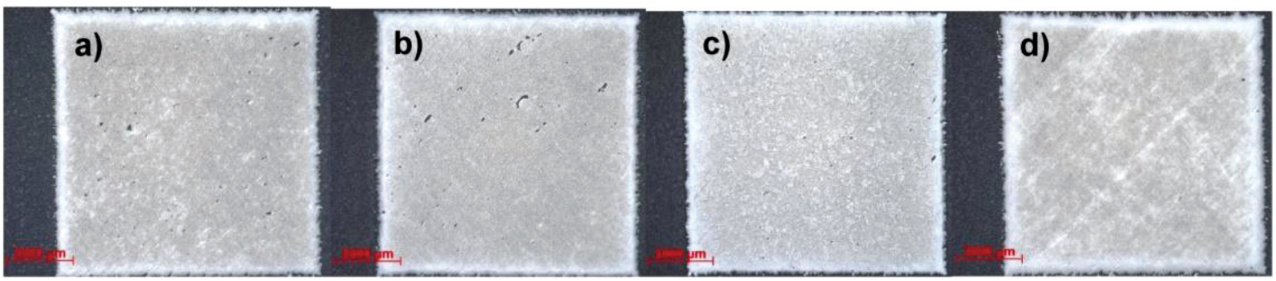

Figure 2: Optical microscopy images of 3D-printed Ti-6Al-4V samples observed at 12.5× magnification

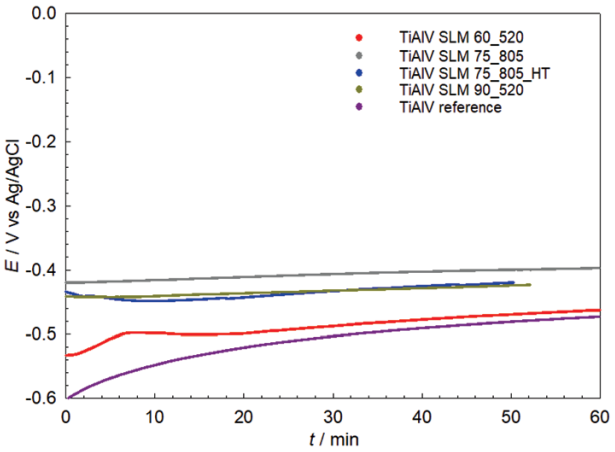

Figure 3: Open-circuit potential measurement for the Ti-6Al-4V samples (SLM produced with various parameters and reference sample) in artificial saliva at 37 °C

lowest relative density was measured for the specimen SLM-90-520 with the lowest porosity. It can be assumed that the relative density is strongly related to the surface roughness and not so much to the internal porosity of the specimens. The relative density of the other two specimens (SLM-75-805 and SLM-60-520) was in between the previously mentioned two specimens.

The Vickers hardness was measured as well. This depends on the microstructure, since there are two distinctive HV values, i.e., for a sample that was heat treated it was lower at (318 ± 25) HV, but for the other SLM-printed sample it was higher and with similar values at (393 ± 26) HV and (394 ± 25) HV for SLM-60-520 and SLM-75-805, respectively. However, the specimen SLM-90-520 printed with the highest laser energy density has the highest hardness, which is very probably the result of the highest temperature difference between the melted surface and the environment, and subsequently the fastest cooling rate.

Table 2: Vickers hardness and porosity values for 3D-printed Ti-6Al-4V samples

Ti-6Al-4V sample	Porosity (%)	Density (g/cm^3)	HV 0.3
SLM-60-520	0.4	4.364 ± 0.022	393 ± 26
SLM-75-805	0.5	4.357 ± 0.054	394 ± 25
SLM-75-805-HT (heat treated)	0.1	4.389 ± 0.038	318 ± 25
SLM-90-520	0.1	4.333 ± 0.033	420 ± 26

3.2 Open-circuit potential measurements

Corrosion studies included a measurement of the open-circuit potential, a linear polarization measurement, the electrochemical impedance spectroscopy and potentiodynamic measurements. The results of the linear polarization measurements are not presented in this study.

When the Ti-6Al-4V samples were immersed in artificial saliva at 37 °C, the potential slowly started to increase (**Figure 3**). The increase in potential upon exposure to the saliva indicates the growth of a passive layer. The lowest potential was measured for the reference Ti-6Al-4V sample, reaching a value of –0.50 V after 1 h of exposure time, with very similar value for SLM-60-520, i.e., –0.46 V.

The most positive OCP potential of the SLM-fabricated SLM-75-805 was at –0.397 V after 1 h of exposure in saliva at 37 °C. The SLM-fabricated samples with a higher or lower laser power (SLM-90-520) had a more negative potential (between the reference and the SLM-75-805 fabricated sample) after 1 h of exposure to artificial saliva at 37 °C. The small potential change during the exposure of the TiAlV alloy to simulated saliva points to a relatively stable process observed between the Ti oxide and the artificial saliva.

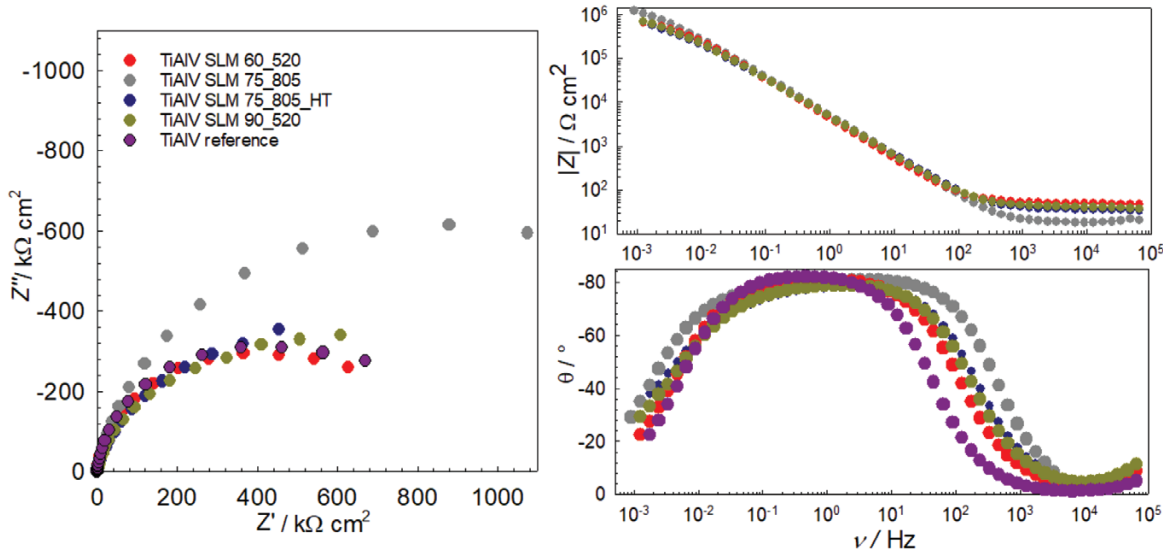

Figure 4: Nyquist and Bode plots of Ti-6Al-4V (reference and SLM samples, printed with different parameters) in simulated saliva at 37 °C

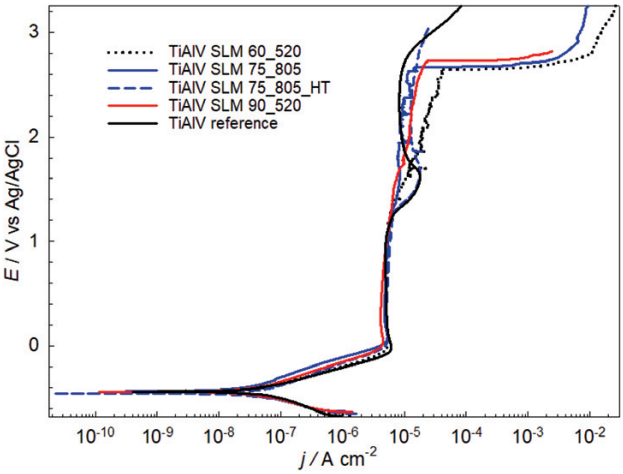

Figure 5: Potentiodynamic curves for the SLM-fabricated Ti-6Al-4V samples and Ti-6Al-4V reference sample in artificial saliva at 37 °C, scan rate 1 mV/s

3.3 Electrochemical impedance measurement

The electrochemical impedance measurements (EIS) were taken once the steady state was reached (**Figure 4**). It can be observed that the impedance responses for the Ti-6Al-4V reference and SLM samples are different. The highest impedance response was measured for the SLM-75-805, where the absolute impedance at the lowest measured frequency was 1.27 MΩ·cm^2. This particular sample also had the highest porosity of 0.5 %. A higher porosity resulted in a larger specific area and thus a higher value of the impedance response. A similar observation was reported earlier, where the high porosity was reflected in the higher corrosion-resistance values of the CoCr alloys as well.[22] The thermally treated (SLM-75-805-HT) sample had the lowest absolute impedance at 0.577 MΩ·cm^2. The reference Ti-6Al-4V sample had an absolute impedance value of 0.724 MΩ·cm^2.

The sample with the second-highest porosity of 0.4 %, printed with low laser power of 60 W and a speed scan of 520 mm/s resulted in absolute impedance value at 0.678 MΩ·cm^2, while the specimen printed at the highest laser-power density SLM-90-520 had similar absolute impedance value of 0.697 MΩ·cm^2.

Minor differences can be observed from the EIS results, but no distinctive difference could be revealed when the SLM-printed samples were compared to the reference wrought alloy of Ti-6Al-4V. The differences were related to the presence of pores and not directly correlated to the laser energy density of the studied samples. Microstructural changes of the heat-treated sample resulted in a lower corrosion resistance.

3.3 Potentiodynamic polarization measurement

Potentiodynamic curves for the reference material and the SLM-printed Ti-6Al-4Al alloy are given in **Figure 5** and the electrochemical parameters are extracted in **Table 3**. The corrosion potential, E_{corr}, was similar in all the samples. The values of the corrosion-current density, j_{corr}, were also similar for all the samples, with values between 25.8 nA/cm^2 and 58.4 nA/cm^2.

Potentiodynamic curves for the studied samples had similar cathodic behavior. In the anodic region, passive behavior was observed with a constant passive-current density of the order of 4–5 μA/cm^2, similar for all the samples up to 1.2 V. Then, some differences in the anodic behavior were observed. Namely, for the reference Ti-6Al-4V and the heat-treated sample 75-805-HT, an anodic peak was observed, which showed similarities between these two samples. That might be due to the fact that the microstructures of these two specimens do not contain α' martensitic phase, but $\alpha + \beta$. A similar current peak was observed in the survey of Aziz-Kerrzo for a Ti-6Al-4V alloy.[10] From the literature, there is no consensus as to which microstructure of this alloy has the best corrosion properties (martensitic α' or $\alpha + \beta$). How-

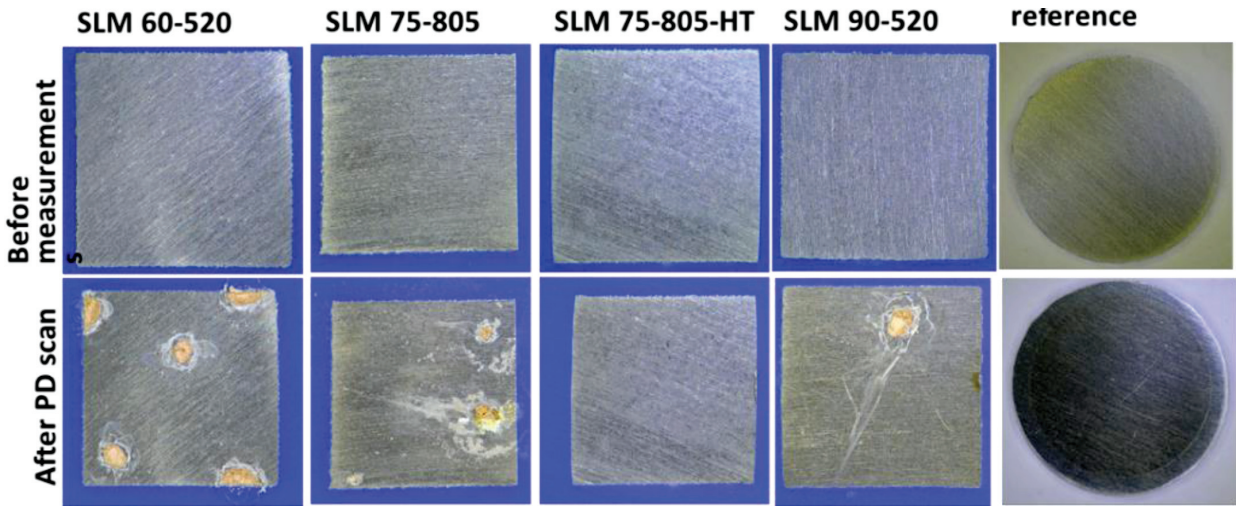

Figure 6: Optical microscopy of the type and extent of the corrosion damage on the samples following the potentiodynamic experiments

Table 3: Corrosion potential, corrosion current density for different Ti-6Al-4V samples obtained from open-circuit potential measurement and potentiodynamic polarization

Ti-6Al-4V sample	E_{OCP}/V	E_{corr}/V	j_{corr}/(nA·cm^{-2})	E_b/V	ΔE (E_b–E_{corr})/V
SLM 60-520	–0.464	–0.453	51.7	2.61	3.05
SLM-75-805	–0.397	–0.445	25.6	2.68	3.11
SLM-75-805-HT (heat treated)	–0.424	–0.461	58.4	3.03	3.49
SLM-90-520	–0.424	–0.430	41.1	2.73	3.17
Ti-6Al-4V-reference	–0.50	–0.445	49.0	2.75	3.19

ever, in the literature we found that between α lamelles and β plates in $\alpha + \beta$ microstructure the galvanic effect could affect the preferential corrosion of the β-phase.[23] In addition, martensitic α' microstructure enables the formation of a more homogenous passive layer than the $\alpha + \beta$, and thus a better corrosion performance.[24]

3.3 Optical microscopy

Following the potentiodynamic (PD) scans, the surfaces exposed to artificial saliva were inspected. As observed from the images after the PD scans, defects in the form of spots can be seen.

The 3D-printed sample with a higher porosity (SLM-60-520 and SLM-77-805) showed the highest number of spots with a discoloured surface in **Figure 6**. One spot was found on the SLM-90-520 specimen, and no spots are present after the PD measurements on the SLM-75-805-HT and the reference specimens.

4 CONCLUSIONS

This research investigated a Ti-6Al-4V dental alloy in artificial saliva at 37 °C. Different forms of Ti-6Al-4V alloy were studied, i.e., three samples made from Ti-6Al-4V powder using the selective laser melting (SLM) method, one sample being also thermally treated and compared to a reference Ti-6Al-4V alloy.

The microstructural, physical and corrosion studies showed that:

1) All the SLM-printed samples contained a certain amount of porosity, whereas the reference sample did not. The high porosity is related to the printing parameters with lower laser energy density. The higher energy density and heat treatment resulted in a lower micro-porosity.
2) After 1 h of immersion in the artificial saliva the corrosion potential was more positive in the SLM-printed Ti-6Al-4V samples when compared to the reference sample.
3) Electrochemical impedance spectroscopy measurements and potentiodynamic measurements showed complementary electrochemical properties; the reference and heat-treated samples had very similar properties observed by potentiodynamic scans, while the EIS showed diverse properties due to different levels of porosity.
4) When comparing the hardness of the different SLM-fabricated Ti-6Al-4V samples, the heat-treated sample had a lower hardness due to the globular microstructure consisting of $\alpha + \beta$. The highest porosity was measured for the SLM-90-520 specimen, printed with the highest laser-power density and it can be contributed to the highest cooling rate due to the highest temperature difference.
5) Due to the characteristics of the printed samples it can be concluded that metal frameworks fabricated by SLM technology in clinical practice are suitable for long-span bridges in fixed prosthodontics.

Acknowledgments

The financial support of the Slovenian Research Agency (SRA), under grant No L2-1831, is hereby gratefully acknowledged. Great thanks to Tanja Antič for preparing the metallographic specimen and Jošt Oblak for performing electrochemical experiments. The financial support of Itmedika, Prodent, Dentalia, AO American Orthodontics, Dentas, Zavod MD-RI Institut za raziskavo materialov v medicini is greatly acknowledged.

5 REFERENCES

[1] P. A. Schweitzer, Fundamentals of metallic corrosion: Atmospheric and Media Corrosion of Metals, Corrosion Engineering Handbook, 2nd ed., CRC press, Taylor&Francis Group, NY, 2007

[2] D. Williams, Chapter 9 - Biocompatibility, Tissue Engineering, Academic Press (2008) 255–278, doi:10.1016/B978-0-12-370869-4.00009-4

[3] M. Niinomi, Metals for Biomedical Devices, 2nd ed., Woodhead Publishing Limited, Cambridge, UK, 2019

[4] M. M. Methani, P. F. Cesar, R. B. de Paula Miranda, S. Morimoto, M. Özcan, M. Revilla-León, Additive Manufacturing in Dentistry: Current Technologies, Clinical Applications, and Limitations, Curr. Oral Health Rep., 7 (**2020**), 327–334, doi:10.1007/s40496-020-00288-w

[5] M. Abdel-Hady Gepreel, M. Niinomi, Biocompatibility of Ti-alloys for long-term implantation, Journal of the Mechanical Behavior of Biomedical Materials, 20 (**2013**), 407–415, doi:10.1016/j.jmbbm.2012.11.014

[6] A. Cigada, M. Cabrini, P. Pedeferri, Increasing of the corrosion resistance of the Ti-6Al-4V alloy by high thickness anodic oxidation. Journal of Materials Science: Materials in Medicine, 6 (**1992**) 3, 408–412, doi:10.1007/bf00701236

[7] I. Milošev, M. Metikos-Huković, H. H. Strehblow, Passive film on orthopaedic TiAlV alloy formed in physiological solution investi-

gated by X-ray photoelectron spectroscopy, Biomaterials, 21 (**2000**), 2103–2113, doi:10.1016/s0142-9612(00)00145-9

[8] S. Barril, S. Mischler, D. Landolt, Electrochemical effects on the fretting corrosion behaviour of Ti-6Al-4V in 0.9% sodium chloride solution, Wear, 259 (**2005**), 282–291, doi:10.1016/j.wear.2004.12.012

[9] I. Milošev, B. Kapun,V. S. Šelih, The effect of fluoride ions on the corrosion behaviour of Ti metal, and Ti6–Al–7Nb and Ti–6Al–4V alloys in artificial saliva, Acta Chim. Slov., 60 (2013) 543–555

[10] M. Aziz-Kerrzo, K. G. Conroy, A. M. Fenelon, S. T Farrell, C. B. Breslin, Electrochemical studies on the stability and corrosion resistance of titanium-based implant materials, Biomaterials, 22 (2001), 1531–1539

[11] J. Pan, D. Thierry, C. Laygraf, Electrochemical impedance spectroscopy study of passive oxide film on titanium for implant application, Electrochim. Acta, 41 (**1996**), 1143–1153, doi:10.1016/0013-4686(95)00465-3

[12] I. Milošev, T. Kosec, H. H. Strehblow, XPS and EIS study of the passive film formed on orthopaedic Ti–6Al–7Nb alloy in Hank's physiological solution, Electrochim. Acta, 53 (**2008**), 3547–3558, doi:10.1016/j.electacta.2007.12.041

[13] A. Sobolev, I. Wolicki, A. Kossenko, M. Zinigrad, K. Borodianskiy, Coating Formation on Ti-6Al-4V Alloy by Micro Arc Oxidation in Molten Salt, Materials, 11 (**2018**) 9, 1611, doi:10.3390/ma11091611

[14] A. R. Ribeiro, F. Oliveira, L. C. Boldrini, P. E. Leite, P. Falagan-Lotsch, A. B. R. Linhares, W. F. Zambuzzi, B. Fragneaud, A. P. C. Campos, C. P. Gouvêa, B. S. Archanjo, C. A. Achete, E. Marcantonio, L. A. Rocha, J. M. Granjeiro, Micro-arc oxidation as a tool to develop multifunctional calcium-rich surfaces for dental implant applications, Materials Science and Engineering: C, 54 (**2015**), 196–206, doi:10.1016/j.msec.2015.05.012

[15] X. Liu, S. Chen, J. Tsoi, J. P. Matinlinna, Binary titanium alloys as dental implant materials-a review, Regenerative biomaterials, 4 (**2017**) 5, 315–323, doi:10.1093/rb/rbx027

[16] M. Niinomi, M. Nakai, J. Hieda, Development of new metallic alloys for biomedical applications, Acta Biomaterialia, 8 (**2012**), 3888–3903, doi:10.1016/j.actbio.2012.06.037

[17] N. Yumak, K. Aslantaş, A review on heat treatment efficiency in metastable β titanium alloys: the role of treatment process and parameters, Journal of Materials Research and Technology, 9 (**2020**), 15360–15380, doi:10.1016/j.jmrt.2020.10.088

[18] ISO 6507-1: 2018, Metallic materials — Vickers hardness test — Part 1: Test method

[19] G. S. Duffo, E. Q. Castillo, Development of artificial saliva solution for studying the Corrosion Behavior of Dental Alloys, Corrosion, 60 (**2004**), 594–602, doi:10.1016/j.electacta.2012.05.1

[20] ASTM E2109-01, Standard test methods for determining area percentage porosity in thermal sprayed coatings, doi:10.1520/E2109-01R14

[21] T. Kosec, M. B. Leban, M. Kurnik, I. Kopač, Comparison of the corrosion properties of CoCrMo dental alloys in artificial saliva (Primerjava korozijskih lastnosti CoCrMo dentalnih zlitin v umetni slini), Materiali in tehnologije, 55 (**2021**) 6, 819–824, doi:10.17222/mit.2021.283d

[22] M. Atapour**,** A. Pilchak, G. S. Frankel, J. C. Williams, M. H. Fathi, M. Shamanian, Corrosion Behavior of Ti-6Al-4V with different thermomechanical treatments and microstructure, Corrosion, 66 (**2010**) 6, 065004–065009, doi:10.5006/1.3452400

[23] P. Bocchetta, L.-Y. Chen, J. D. C. Tardelli, A. C. dos Reis, F. Almeraya-Calderón, P. Leo, Passive layers and corrosion resistance of biomedical Ti-6Al-4V and β-Ti alloys, Coatings, 11 (**2021**) 5, 487, doi:10.3390/coatings11050487

[24] S. Pal, M. Finšgar, T. Bončina, G. Lojen, T. Brajlih, I. Drstvenšek Effect of surface powder particles and morphologies on corrosion of Ti-6Al-4 V fabricated with different energy densities in selective laser melting. Materials & Design, 211 (**2021**), 110184, doi:10.1016/j.matdes.2021.110184